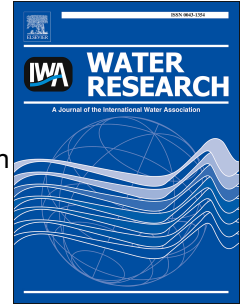


# Accepted Manuscript

Spatiotemporal Patterns and Source Attribution of Nitrogen Load in a River Basin with Complex Pollution Sources

Xiaoying Yang, Qun Liu, Guangtao Fu, Yi He, Xingzhang Luo, Zheng Zheng



PII: S0043-1354(16)30099-9

DOI: [10.1016/j.watres.2016.02.040](https://doi.org/10.1016/j.watres.2016.02.040)

Reference: WR 11856

To appear in: *Water Research*

Received Date: 28 September 2015

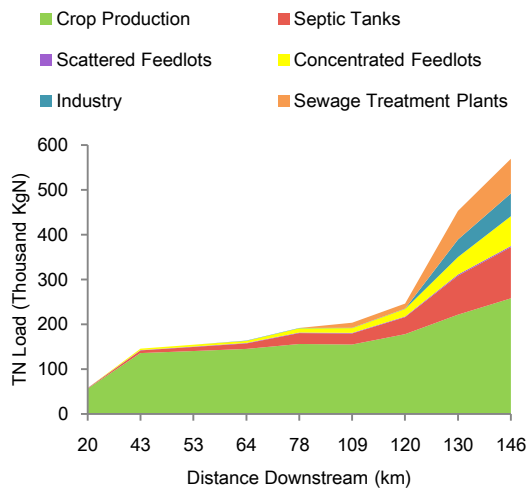
Revised Date: 14 February 2016

Accepted Date: 15 February 2016

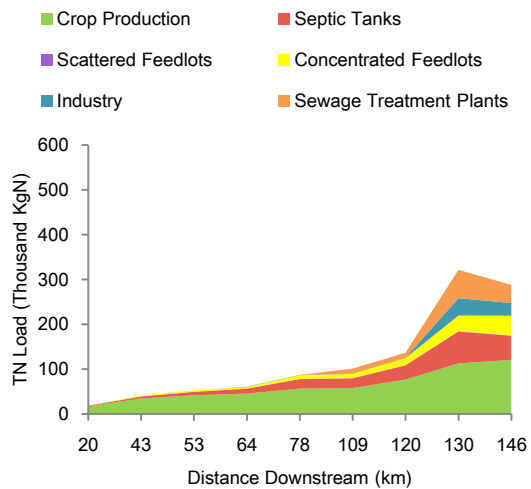
Please cite this article as: Yang, X., Liu, Q., Fu, G., He, Y., Luo, X., Zheng, Z., Spatiotemporal Patterns and Source Attribution of Nitrogen Load in a River Basin with Complex Pollution Sources, *Water Research* (2016), doi: [10.1016/j.watres.2016.02.040](https://doi.org/10.1016/j.watres.2016.02.040).

This is a PDF file of an unedited manuscript that has been accepted for publication. As a service to our customers we are providing this early version of the manuscript. The manuscript will undergo copyediting, typesetting, and review of the resulting proof before it is published in its final form. Please note that during the production process errors may be discovered which could affect the content, and all legal disclaimers that apply to the journal pertain.

Average Monthly TN Load in Summer



Average Monthly TN Load in Winter



1 Spatiotemporal Patterns and Source Attribution of Nitrogen Load in a River Basin with  
2 Complex Pollution Sources

3 Xiaoying Yang,<sup>1\*</sup> Qun Liu,<sup>2</sup> Guangtao Fu,<sup>3</sup> Yi He,<sup>4</sup> Xingzhang Luo,<sup>1</sup> and Zheng Zheng<sup>1</sup>

4 <sup>1</sup>Department of Environmental Science and Engineering, Fudan University, Shanghai  
5 200433, China.

6 <sup>2</sup>Zhumadian City Bureau of Environmental Protection, Zhumadian 463000, China

7 <sup>3</sup>Centre for Water Systems, College of Engineering, Mathematics and Physical Sciences,  
8 University of Exeter, Exeter, United Kingdom, EX4 4QF

9 <sup>4</sup>Tyndall Centre for Climate Change Research, School of Environmental Sciences,  
10 University of East Anglia, Norwich, United Kingdom, NR4 7TJ

11 \*Email: xiaoying@fudan.edu.cn

12 **ABSTRACT**

13 Environmental problems such as eutrophication caused by excessive nutrient discharge  
14 are global challenges. There are complex pollution sources of nitrogen (N) discharge in  
15 many river basins worldwide. Knowledge of its pollution sources and their respective  
16 load contributions is essential to developing effective N pollution control strategies. N  
17 loads from all known anthropogenic pollution sources in the Upper Huai River basin of  
18 China were simulated with the process-based SWAT (Soil and Water Assessment Tool)  
19 model. The performances of SWAT driven by daily and hourly rainfall inputs were  
20 assessed and it was found that the one driven by hourly rainfall outperformed the one  
21 driven by daily rainfall in simulating both total nitrogen (TN) and ammonia nitrogen  
22 ( $\text{NH}_4\text{-N}$ ) loads. The hourly SWAT model was hence used to examine the spatiotemporal  
23 patterns of TN and  $\text{NH}_4\text{-N}$  loads and their source attributions. TN load exhibited  
24 significant seasonal variations with the largest in summer and the smallest in spring.  
25 Despite its declining proportion of contribution downstream, crop production remained

26 the largest contributor of TN load followed by septic tanks, concentrated animal feedlot  
27 operations (CAFOs), municipal sewage treatment plants, industries, and scattered  
28 animal feedlot operations (SAFOs). There was much less seasonal variation in  $\text{NH}_4\text{-N}$   
29 load. CAFOs remained the largest source of  $\text{NH}_4\text{-N}$  load throughout the basin, while  
30 contributions from industries and municipal sewage treatment plants were more evident  
31 downstream. Our study results suggest the need to shift the focus of N load reduction  
32 from “end-of-pipe” sewage treatment to an integrated approach emphasizing  
33 stakeholder involvement and source prevention.

34 **KEY WORDS**

35 nitrogen load, spatiotemporal pattern, pollution source attribution, SWAT, hourly  
36 rainfall, Huai River

## 37 1. Introduction

38 Nitrogen (N) is arguably the most important nutrient in regulating primary  
39 productivity and species diversity in both aquatic and terrestrial ecosystems (Vitousek *et*  
40 *al.*, 2002). The ecological implications of human alterations to the N cycle have been  
41 profound as human activities have already significantly altered the global N cycle. From  
42 1860 to the early 1990s, anthropogenic creation of reactive N compounds increased  
43 globally from approximately 15 to 156 Tg N y<sup>-1</sup> (Galloway *et al.*, 2004). Human  
44 conversion of N<sub>2</sub> to more reactive N species has caused a wide range of environmental  
45 problems, ranging from effects on atmospheric chemistry, deterioration of freshwater  
46 quality, marine eutrophication, to declines in biodiversity (Henriksen *et al.*, 1997;  
47 Howarth, 2008; Pastuszak *et al.*, 2014).

48 The intensity and spatial variation of N loads into river basins depends on a number  
49 of natural as well as anthropogenic factors. The natural factors include land use/land  
50 cover types, soil types, meteorological, geological, hydrological conditions, and etc. The  
51 anthropogenic factors include emissions from various pollution sources, the operating  
52 pollutant removal facilities, and the implemented best management practices (Lepisto *et*  
53 *al.*, 2006; Pastuszak *et al.*, 2014; Gallo *et al.*, 2015). The various rates, frequencies, and  
54 locations of N discharge as well as the diverse influencing factors of N transport and  
55 transformation make it very challenging to quantify each pollution source's N load  
56 contributions, especially in those river basins with complex pollution sources but  
57 limited data on pollution sources and N concentrations in water environment.

58 China is faced with the severe challenge of widespread eutrophication due to the  
59 excessive discharge of nutrients such as N. Many studies as well as its first national  
60 pollution census have indicated that non-point source pollution has played an  
61 increasingly significant role in water quality deterioration in China (Xu *et al.*, 2009; Liu

62 *et al.*, 2013; Li *et al.*, 2014). Previous studies on non-point source pollution have been  
63 mostly focusing on agricultural runoff (Duncan, 2014; Guo *et al.*, 2014; Panagopoulos  
64 *et al.*, 2014; Yun *et al.*, 2015). Nevertheless, the composition of non-point pollution  
65 sources is usually more complex (Li *et al.*, 2014). In China, for example, more than 50  
66 percent of its 1.3 billion population live in rural areas, where domestic sewage from  
67 rural households is hardly treated before being discharged into the environment. In  
68 addition, with rapid economic development and the subsequent improvement in  
69 people's living standards, there is an ever-growing appetite for meat and dairy  
70 consumption in the country. In response to this are the burgeoning animal feeding  
71 operations of different sizes, many of which are not equipped with sufficient waste  
72 disposal facilities.

73 River Huai, the third longest river in China, is one of the mostly polluted rivers in  
74 the country. During the past two decades, Chinese government has made tremendous  
75 investment to reverse the trend of deteriorating water quality in the basin, including 16.6  
76 billion RMB on industrial sewage treatment between 1996 and 2000, and 25.6 billion  
77 RMB on municipal sewage treatment between 2001 and 2005. Since 2006, the  
78 government's focus has shifted from reducing the concentrations of discharging  
79 pollutants to reducing their total loads from the sources, with more than 60 billion RMB  
80 spent on cutting pollutant loads in the basin. However, the enormous financial  
81 investment has yet to bring about the much anticipated improvement in the water  
82 quality of the basin. For example, five categories of water bodies have been specified in  
83 the Chinese Surface Water Quality Standard (GB3838-2002). Among them, Category  
84 IV water could only be used for industrial production or human amusement without  
85 direct body contact, while Category V water could only be used for agriculture or  
86 scenery. The 2013 annual report of China's environment quality conditions by Chinese

87 Ministry of Environment Protection stated that water quality fell between category IV  
88 and V of the National Surface Water Quality Standard (GB 3838-2002) at 34.7% of the  
89 95 routine monitoring sites along the River Huai, and below Category V at 17.9% of the  
90 monitoring sites.

91 Knowledge of pollution sources and their respective load contributions is the  
92 prerequisite to the development of cost-effective pollution control programs and  
93 optimization of pollution control strategies (Lindgren *et al.*, 2007; Carpenter, 2008) in a  
94 river basin. The pollution sources can be very complex that include rural households,  
95 crop production, animal feedlot operations, municipal sewage treatment plants, and  
96 industries. Previous studies have been mostly resorting to a variety of empirical  
97 coefficient methods to estimate pollution loads from various sources (Chen *et al.*, 2013;  
98 Liu *et al.*, 2013; Shen *et al.*, 2013; Delkash *et al.*, 2014). Not only is it difficult to  
99 validate the adopted empirical coefficients, the coefficient methods also fail to account  
100 for the migration and transformation of the pollutants from the points of discharge to the  
101 final receiving water bodies.

102 A number of dynamic process-based models such as the Soil and Water Assessment  
103 Tool (SWAT) (Arnold *et al.*, 2014; Gassman *et al.*, 2014) , the Hydrological Simulation  
104 Program–FORTRAN (HSPF) (Nasr *et al.*, 2007; Xie and Lian, 2013), the Integrated  
105 Nutrients in Catchments-Nitrogen (INCA-N) model (Rankinen *et al.*, 2006; Wade *et al.*,  
106 2006), the Annualized Agricultural Nonpoint Source (AnnAGNPS) model (Pease *et al.*,  
107 2010; Que *et al.*, 2015), and the HBV-NP (Andersson *et al.*, 2005; Lindstrom *et al.*,  
108 2005) have been developed and used for modeling N loads in river basins. SWAT is  
109 selected in this study due to its open source feature and wide user communities, as well  
110 as its ability for simulating the pollutant transport processes from various point and  
111 non-point pollution sources in a river basin. Nevertheless, SWAT has been

112 predominantly used to study non-point source pollution from agricultural fields (Zhang  
113 *et al.*, 2013; Cerro *et al.*, 2014; Jiang *et al.*, 2014; Ouyang *et al.*, 2014; Zhang *et al.*,  
114 2014) despite its capabilities of incorporating a variety of pollution sources such as  
115 point sources and septic tanks (Oliver *et al.*, 2014). The ignorance of the point sources  
116 and septic tanks in the process-based models may lead to the overestimation of the  
117 relative contributions from diffusive sources such as agriculture and the disproportional  
118 targeting of potential pollution sources (Withers *et al.*, 2012).

119 The majority of water quality modeling studies, including those using SWAT, have  
120 used monthly or daily meteorological inputs to drive the models. However,  
121 meteorological inputs at different temporal resolutions, especially precipitation, could  
122 result in different simulations of hydrological responses and hence pollutant transport  
123 and transformation processes (Yang *et al.*, 2015). There is a need for deeper  
124 understandings of the impacts of the temporal resolution of precipitation on the  
125 process-based models' simulations of pollutant transport and transformation processes.  
126 In view of the gaps, the research objectives of this study are to (1) establish the SWAT  
127 model to simulate the N discharge and transport processes from all known  
128 anthropogenic point and non-point pollution sources in a river basin with complex  
129 pollution sources, (2) compare the SWAT models with daily and hourly rainfall inputs in  
130 their N pollution simulation performances, and (3) quantify the N load contributions  
131 from each pollution source and analyze their spatiotemporal patterns in a river basin.

132 This study differs from previous works using SWAT to simulate N loads in the  
133 following ways:

- 134 1. We used SWAT to simulate N discharge and transport processes from all known  
135 anthropogenic sources in a large river basin including crop production,  
136 scattered small-scale animal feedlot operations, rural household septic tanks,



137 industries, municipal sewage treatment plants, and concentrated animal feedlot  
138 operations.

139 2. We evaluated the impacts of the temporal resolution of rainfall inputs on the  
140 SWAT models' performance in both stream discharge and N load simulations in  
141 a large river basin.

142 3. We analyzed the spatiotemporal patterns of both total nitrogen (TN) and  
143 ammonia nitrogen (NH<sub>4</sub>-N) load contributions from each of the six pollution  
144 sources. Each pollution source's seasonal TN and NH<sub>4</sub>-N load contributions  
145 were analyzed and compared at nine locations along the main reach of the  
146 study region.

## 147 **2. Materials and methods**

### 148 **2.1. Study region**

149 The Ru River Basin lies upstream of the Huai River Basin and is selected as the  
150 study region. The River Ru originates from the Banqiao reservoir and runs for  
151 approximately 223 km passing through nine counties and one district of the Zhumadian  
152 City. The outlet of the Ru River Basin is located at the Shakou hydrological station. The  
153 study region completely falls within the administrative boundary of the Zhumadian City  
154 with a drainage area of 5803 km<sup>2</sup> (Fig. 1).

155 The study region is predominantly agricultural with farmland, wood land, grassland,  
156 and rural residential areas accounting for 65.6%, 14.5%, 5.1%, and 8.7% of its land  
157 coverage, respectively. Mostly hilly in the west and flat in the east, its surface elevation  
158 ranges from less than 50 m to nearly 1000 m. Located in the transition zone between the  
159 northern subtropical climate and warm temperate climate, the region has four distinctive  
160 seasons with annual mean temperature around 15°C and precipitation around 900 mm.  
161 Heavily influenced by monsoon, precipitation in the region mostly occurs in the

162 summer months from June to August.

163 Due to its favorable weather conditions and large extent of flat terrain, the region  
164 has traditionally been a main supplier of grain and meat products in China. In 2010, for  
165 example, the city of Zhumadian was reported to have a rural population of 5.08 million,  
166 producing 6.49 million tons of grains and 0.78 million tons of meat. Meanwhile, the city  
167 has substantial industrial activities with a gross industrial product value of 39.3 billion  
168 RMB in 2010. The industrial, agricultural, and domestic activities have contributed to  
169 significant water quality deterioration in the region. The water quality of the Banqiao  
170 reservoir, the origin of the River Ru, could meet the category III of the GB 3838-2002  
171 Standard, allowing it to serve as a drinking water source for the local community. At the  
172 downstream Shakou hydrological station, however, its water quality deteriorates sharply.  
173 With annual mean total nitrogen (TN) concentration increasing to 3.93 mg/l in 2010, it  
174 even fails to meet the category V of the Standard. Understanding how various pollution  
175 sources contribute to the considerable increase in N concentration is the prerequisite to  
176 developing effective water pollution control programs in the region.

## 177 **2.2 Data Sources**

178 The land use and land cover (LULC) data in 2005 was obtained from the Chinese  
179 Academy of Sciences, which was further classified into the standard LULC categories  
180 of SWAT. The soil types and properties were mostly extracted from the soil databases  
181 of Nanjing Institute of Soil Science (Yu *et al.*, 2007a; Yu *et al.*, 2007b; Shi *et al.*, 2010),  
182 except that the available water capacity and soil carbon content were estimated using  
183 the SPAW (Soil – Plant – Atmosphere – Water) software (Saxton and Willey, 2005),  
184 and the soil nutrient contents (nitrate, organic nitrogen, labile phosphorous, and organic  
185 phosphorous) were obtained from the local soil survey reports. Table 1 summarized the  
186 required data inputs for the SWAT model and their sources.

187 The 25m Digital Elevation Model (DEM) data was used to delineate the sub-basins.  
188 With a threshold area of 8000 ha, a total of 55 sub-basins were delineated (Fig. 1),  
189 which were further divided into 394 hydrological response units (HRUs). Each HRU  
190 represents homogeneous characteristics of LULC, soils, and slopes. The residential  
191 medium/low density (URML) areas that represent rural residential areas were all  
192 retained during HRU delineation for simulating N load from rural septic tanks.

193 Daily records of maximum and minimum temperature, sunshine hours, relative  
194 humidity, and wind speed at the Zhumadian weather station from 2001 to 2011 were  
195 acquired from the China Meteorological Administration. Daily sunshine hours were  
196 converted to daily solar radiation using the Angstrom-Prescott equation (Prescott, 1940)  
197 with empirical parameters from Zuo et al. (1963). Daily and hourly rainfalls at 28  
198 rainfall stations from 2001 to 2011 were obtained from the Hydrological Yearbooks  
199 compiled by the Ministry of Water Resources of China. Daily streamflows and the  
200 subsequently derived monthly streamflows at three hydrological stations (Lixin,  
201 Luzhuang, and Shakou) and daily outflow from three major reservoirs (Banqiao,  
202 Boshan, and Suyahu) from 2005 to 2011 were also obtained from the reports (see Fig. 1  
203 for the locations of the three stations and reservoirs).

204 Monthly observations of TN and ammonia nitrogen ( $\text{NH}_4\text{-N}$ ) concentrations at the  
205 Shakou station from 2006 to 2011 were obtained from the Bureau of Environmental  
206 Protection of the Zhumadian City. Between 2006 and 2008, TN concentrations were  
207 only monitored in the odd numbered months. Monthly TN and  $\text{NH}_4\text{-N}$  concentrations  
208 were multiplied by monthly streamflows to estimate their monthly loads, respectively.  
209 Both point and non-point pollution sources are responsible for the deteriorating water  
210 quality in the study region. Point sources include industries, municipal sewage treatment  
211 plants, and concentrated animal feedlot operations (CAFOs). Non-point pollution

212 sources include crop production, scattered small-scale animal feedlot operations  
213 (SAFOs), and rural households. Annual N emissions from industries and CAFOs were  
214 extracted from the database of 2010 census of pollution sources in the Zhumadian City.  
215 N emissions from six municipal sewage treatment plants in 2010 were obtained from  
216 the Bureau of Environmental Protection of the Zhumadian City. Total N emissions from  
217 industries, CAFOs, and municipal sewage treatment plants were summarized for the 21  
218 sub-basins with the presence of point sources (Fig. 1), and their mean monthly loads  
219 were used as point source inputs in SWAT.

220 Face-to-face interviews with 116 randomly selected farmers from 16 villages in the  
221 study region were conducted to collect information on current crop management  
222 practices. Our interview results indicated that most of the agricultural fields in the  
223 region were under the wheat-corn rotation (June to September for growing corn and  
224 October to next May for growing wheat) with fairly homogeneous crop management  
225 practices as summarized in Table 2.

226 Rural population of the nine counties and one district located fully or partially in  
227 the study region was obtained from the Statistical Yearbook of the Zhumadian city. The  
228 rural population density of each sub-basin was estimated as the area-weighted average  
229 of county rural population densities, based on which the rural population of its HRUs  
230 containing URML was calculated.

231 Like many other regions in China, rural domestic sewage has not been collected for  
232 central treatment in the study region. Conventional septic tanks are the main facilities  
233 for rural sewage treatment. Based on previous studies of the characteristics of rural  
234 household sewage discharge and the pollutant removal efficiencies of septic tanks in  
235 China, the septic tank effluent flow rate was set to be 50 l/d per capita, and the TN  
236 concentration of the septic tank effluent was set to be 90 mg/l in the SWAT model

237 (WANG *et al.*, 2008; Xu *et al.*, 2008; WANG *et al.*, 2010; Hou *et al.*, 2012).

238 County level N emissions from SAFOs in 2010 were obtained from the Bureau of  
 239 Animal Husbandry of the Zhumadian City, which was converted to the equivalent  
 240 amount of pig manure based on the average ammonia content of 2.57%. N loads from  
 241 SAFOs were estimated by assuming that the equivalent amount of pig manure was  
 242 applied uniformly to crop fields within each county. Each sub-basin's pig manure  
 243 application rate was estimated as the area-weighted average of the county application  
 244 rates.

### 245 **2.3 SWAT Model Development**

246 Both daily and hourly rainfall data were used as inputs for the SWAT models and  
 247 their performances in discharge and N load simulations were compared. The SWAT  
 248 models driven by daily and hourly rainfall are hereinafter referred to as the daily SWAT  
 249 model and the hourly SWAT model, respectively. The Soil and Water Assessment Tool  
 250 Calibration and Uncertainty Procedure (SWAT-CUP) (Abbaspour, 2011) program was  
 251 used for the calibration and validation of the SWAT models. The Nash-Sutcliffe model  
 252 efficiency (NSE) coefficient (Nash and Sutcliffe, 1970) and the coefficient of  
 253 determination ( $R^2$ ) are used as the objective function (see Equations 1 and 2) to evaluate  
 254 the model performance.

$$255 \quad NSE = 1 - \frac{\sum_{i=1}^n (Y_i^{obs} - Y_i^{sim})^2}{\sum_{i=1}^n (Y_i^{obs} - \overline{Y^{obs}})^2} \quad (1)$$

$$256 \quad R^2 = \frac{\left[ \sum_{i=1}^n (Y_i^{obs} - \overline{Y^{obs}}) \sum_{i=1}^n (Y_i^{sim} - \overline{Y^{sim}}) \right]^2}{\sum_{i=1}^n (Y_i^{obs} - \overline{Y^{obs}})^2 \sum_{i=1}^n (Y_i^{sim} - \overline{Y^{sim}})^2} \quad (2)$$

257 where:  $n$  is the total number of observations,  $Y_i^{obs}$  is the value of the observed

258 variable at the  $i$ th time-step,  $Y_t^{sim}$  is the value of the simulated variable at the  $i$ th  
259 time-step, and  $\overline{Y^{obs}}$  and  $\overline{Y^{sim}}$  are the mean of the measured and simulated values.

260 Ranging from 0 to 1,  $R^2$  indicates the percentage of variance in measured data  
261 accounted for by the variance in the simulated results. NSE is a normalized statistic that  
262 describes the degree of the ‘goodness-of-fit’ between model predictions and  
263 observations and can vary between  $-\infty$  and 1, where a value of 1 represents a perfect fit.  
264 It needs to be noted here although the models were driven by daily or hourly  
265 precipitation, their performances of discharge and N load simulations were evaluated at  
266 a monthly time step. Moriasi *et al.* (2007) suggested that the SWAT model evaluated at  
267 a monthly time step should achieve an NSE value of 0.5, 0.65, and 0.75 to be  
268 considered as “satisfactory”, “good”, or “very good”, respectively.

269 The SWAT models were calibrated in two steps. The model parameters associated  
270 with discharge simulations were calibrated first, followed by those associated with N  
271 load simulations. The SUFI-2 algorithm built in the Soil and Water Assessment Tool  
272 Calibration and Uncertainty Procedure (SWAT-CUP) (Abbaspour 2011) was used for  
273 both the calibration and validation of the SWAT models with several iterations of 1000  
274 simulations. In discharge simulation, after the warming-up period from 2001 to 2004,  
275 the SWAT model was calibrated from 2005 to 2007 and validated from 2008 to 2011  
276 based on the monthly streamflow records at the Lixin, Luzhaung, and Shakou  
277 hydrological stations. In N load simulation, both TN and  $\text{NH}_4\text{-N}$  loads at the Shakou  
278 station were used. Because N emissions from many pollution sources were only  
279 available for 2010, the SWAT models for N load simulations were only calibrated for  
280 the period between 2006 and 2011 when monthly TN and  $\text{NH}_4\text{-N}$  concentration data  
281 were available.

282

## 283 2.4 Source Attribution of N Loads

284 Multiple runs of the SWAT model with different scenarios of pollution source  
285 inputs were conducted to estimate the amount of N load from individual pollution  
286 source. As the baseline scenario, the SWAT model was first run without any pollution  
287 source except fertilizer applications on crop fields to estimate the N load from crop  
288 production, denoted as  $Load_{crop}$ . For the other five point and non-point pollution sources,  
289 different SWAT model runs were then carried out to estimate the combined N loads  
290 from crop production and each individual pollution source, whose difference from the  
291 baseline scenario was calculated as the load from individual pollution source. For  
292 example, to calculate the N load from industries, the SWAT model was run only with  
293 industrial N emissions and fertilizer applications, which yielded an estimate of the  
294 combined N load from industries and crop production denoted as  $Load_{crop+ind}$ . N load  
295 contributed by industries could then be simply calculated as  $Load_{crop+ind}-Load_{crop}$ . The  
296 same procedures were repeated to estimate the N load from municipal sewage treatment  
297 plants, CAFOs, SAFOs, and septic tanks, respectively.

## 298 3. Results and discussion

### 299 3.1 Comparison of the daily and hourly SWAT models

300 Table 3 listed the initial range and the calibrated values of the parameters in the  
301 daily and hourly SWAT models for discharge simulation. At the beginning of the  
302 calibration, the same range was used in the calibration of both models. For the  
303 parameter  $Alpha_{BF}$ , its calibration bounding limits were estimated based on the  
304 historical daily discharge records of the hydrological stations using the baseflow filter  
305 program (Arnold and Allen 1999). Comparison between the calibrated daily and hourly  
306 models indicated that the differences in their parameters mainly lay in those related to  
307 surface runoff and groundwater. In the hourly model, its larger  $CN2$  values led to higher

308 surface runoff potentials; its larger *GW\_DELAY* value caused more delay for soil water  
309 to reach the shallow aquifer; and its larger *GW\_REVAP* and lower *REVAPMN* values  
310 enabled more groundwater to diffuse upward and evaporate. These parameter  
311 differences seemed to indicate that the hourly model would predict more surface runoff  
312 and less baseflow contributions than the daily model. However, the two models yielded  
313 opposite water balance analysis results. The daily model gave an estimate of 39%  
314 baseflow contribution to streamflow compared to a larger estimate of 46% by the hourly  
315 model. The difference in water balance estimates could be due to the different runoff  
316 estimation methods used by the two SWAT models. The daily SWAT model used the  
317 SCS curve number method, while the hourly model used the Green & Ampt infiltration  
318 method. In addition, the baseflow filter program gave an estimate of 0.47 for baseflow  
319 contribution, which coincided more with the hourly model results.

320 Table 4 listed the initial range and the calibrated values of the parameters in the  
321 daily and hourly SWAT models for N load simulation. At the beginning of the  
322 calibration, the same range was used in the calibration of both SWAT models.  
323 Comparison between the calibrated values of the parameters of the two models showed  
324 that they mostly fell within a similar range.

325 Table 5 compared the performances of the daily and hourly SWAT models for  
326 simulating discharge and N loads in the study region. Both models were able to simulate  
327 monthly discharge at the three hydrological stations satisfactorily with the NSE  
328 coefficients all above 0.8 and  $R^2$  all above 0.85 for both the calibration and validation  
329 periods. However, there was much difference in their simulations of monthly TN and  
330  $\text{NH}_4\text{-N}$  loads. The NSE statistics of the hourly SWAT model for simulating TN and  
331  $\text{NH}_4\text{-N}$  loads were both 0.82, much higher than 0.63 and 0.58 of the daily model.  
332 According to the criteria suggested by Moriasi et al. (2007), the hourly SWAT model



333 achieved “very good” performance in simulating monthly TN and NH<sub>4</sub>-N loads,  
334 whereas the performance of the daily model could only be considered as “satisfactory”.

335 Fig. 2 compared the observed and simulated TN and NH<sub>4</sub>-N loads by the daily and  
336 hourly SWAT models at the Shakou station for the time period 2006-2011. In general,  
337 the daily SWAT model tended to predict more TN and NH<sub>4</sub>-N loads than the hourly  
338 model, which resulted in a lower NSE value. As shown in Table 4, there was not much  
339 difference in the calibrated values of the parameters directly related to N transport and  
340 transformation process between the daily and hourly SWAT models. The possible  
341 reason for the difference between the two models’ simulations of N load could be due to  
342 their different representations of the hydrological processes in the study region. The  
343 hourly model estimated that baseflow contributed to about 46 % of the total flow, while  
344 the daily model gave an estimate of 39%. Likewise, the ratio of percolation to  
345 precipitation was estimated to be 0.28 in the hourly model, compared to 0.15 in the  
346 daily model. The higher estimate of the baseflow contribution by the hourly model  
347 meant that it predicted more N transport to rivers via the longer and slower path of soil  
348 percolation and groundwater movement, hence allowing more N removal than the  
349 shorter and faster path of surface runoff.

### 350 **3.3 Spatiotemporal analysis and source attributions of N loads**

351 The SWAT model driven by hourly rainfall outperformed the one driven by daily  
352 rainfall, and hence was used to analyze the spatiotemporal patterns of N loads and the  
353 contributions from various pollution sources. Average monthly TN and NH<sub>4</sub>-N loads at  
354 nine sub-basin outlets located along the main reach of the Ru River were compared for  
355 each season (Fig. 3).

356 In the study region, TN load was the highest in summer followed by fall, winter,  
357 and spring, mainly due to the seasonal change in the load from crop production. At the

358 upstream location close to the Banqiao reservoir (comparison point 1), the majority of  
359 the TN load was contributed by crop production, accounting for more than 70% in  
360 spring and more than 90% in the other seasons. The second largest pollution source is  
361 septic tanks, although with much less contribution than crop production, accounting for  
362 29.2% of the TN load in spring and less than 5% in the other seasons. SAFOs  
363 contributed the remaining less than 1% of the TN load throughout the year (Fig. 4).

364 With increasing TN load contributions from other sources downstream, percentage  
365 of TN load from crop production decreased constantly although it remained as the  
366 largest contributor. At around a distance of 120 km downstream (comparison point 7)  
367 before the joining of the tributary of Lianjiang River, which flows through the heavily  
368 urbanized and industrialized Zhumadian urban area, crop production contributed around  
369 70% of the TN load in summer and fall, 56.2% in winter, and 42.9% in spring. Septic  
370 tanks ranked as the second largest contributor of the TN load, accounting for 29.8% in  
371 spring, 23.1% in winter, and around 16% in fall and summer. CAFOs and municipal  
372 sewage treatment plants ranked the third and fourth in their TN load, which accounted  
373 for 15.0% and 10.4% in spring, 11.4% and 8.1% in winter, 8.1% and 5.8% in fall, and  
374 6.8% and 4.6% in summer. Both industries and SAFOs accounted for less than 1% of  
375 the TN load throughout the year (Fig. 4).

376 At the outlet of the Ru river basin (comparison point 9), the percentage of TN load  
377 contributed by crop production dropped to 29.4% in spring, 45.3% in summer, 53.8% in  
378 fall, and 41.9% in winter. Septic tanks remained as the second largest polluter,  
379 contributing 22.8% in spring, 20.0% in summer, 14.8% in fall, and 18.6% in winter. TN  
380 loads from municipal sewage treatment plants and CAFOs were similar, contributing  
381 around 18% in spring, 15% in winter, and 12% in summer and fall. There was a large  
382 increase in the TN load from industries, accounting for 12.1% in spring, 8.9% in

383 summer, 7.8% in fall, and 9.9% in winter. TN load from SAFOs remained below 1%  
384 throughout the year (Fig. 4).

385 The composition of pollution sources for  $\text{NH}_4\text{-N}$  load was very different from TN  
386 (Fig. 5). CAFOs replaced crop production to be the largest source of the  $\text{NH}_4\text{-N}$  load,  
387 followed by industries and municipal sewage treatment plants. Meanwhile, there was  
388 not as much seasonal difference in the  $\text{NH}_4\text{-N}$  load as in the TN load. At the upstream  
389 above the Banqiao reservoir, average monthly  $\text{NH}_4\text{-N}$  load fell below 200 KgN  
390 throughout the year. Before reaching around 120 km downstream, it increased gradually  
391 by receiving loads mainly from CAFOs and later municipal sewage treatment plants. At  
392 the distance of 120 km downstream (comparison point 7), over 70% of the  $\text{NH}_4\text{-N}$  load  
393 came from CAFOs, compared to around 22% from municipal sewage treatment plants,  
394 2% from industries, and 1% from the remaining sources throughout the year. Afterwards,  
395 there was a sharp increase in the  $\text{NH}_4\text{-N}$  load from industries. At the outlet of the Ru  
396 River basin, CAFOs contributed 45.2% of the  $\text{NH}_4\text{-N}$  load in spring, 37.1% in summer,  
397 45.4% in fall, and 49.5% in winter. Industries rose to the second largest source of  
398  $\text{NH}_4\text{-N}$  load, contributing 30.2% in spring, 28.5% in summer, 26.3% in fall, and 26.7%  
399 in winter. Municipal sewage treatment plants ranked third in the  $\text{NH}_4\text{-N}$  load,  
400 contributing 24.5% in spring, 20.4% in summer, 23.4% in fall, and 23.6% in winter.  
401 Crop production contributed to the  $\text{NH}_4\text{-N}$  load mostly in summer and fall, accounting  
402 for 13.0% and 4.4%, respectively. Septic tanks and SAFOs remained as insignificant  
403 sources, contributing less than 1% throughout the year (Fig. 5).

#### 404 **3.4 Comparisons with previous N source attribution studies**

405 Previous process-based modeling studies on N loads have been mostly focused on  
406 agricultural runoff, with some considering loads from municipal and industrial point  
407 sources, and few considering loads from septic tanks and animal feedlot operations. For

408 example, Wu and Chen (2013) used SWAT to investigate the influence of point source  
409 (municipal and industrial sources) and non-point source (agriculture, atmospheric  
410 deposition, and plant residue decomposition) pollution on the water quality of the  
411 Dongjiang River in southern China, and they concluded that agriculture was the  
412 dominant source of N loads.

413 In contrast, quite a few N load studies utilizing export coefficient methods have  
414 encompassed more types of pollution sources. For example, Liu *et al.* (2013) estimated  
415 that rural residential sewage, animal feedlot operations, fertilizer applications, and  
416 industries accounted for 43%, 14%, 10%, and 7% of the N loads to the Lake Tai of  
417 Eastern China. Wang *et al.* (2013) estimated that rural residential sewage, agricultural  
418 activities (including crop production and animal feedlot operations), and industries  
419 accounted for 54%, 34%, and 4% of the TN loads and 66%, 24%, and 5% of the NH<sub>4</sub>-N  
420 loads to the Lake Dianshan of Southern China. HAO *et al.* (2014) estimated that rural  
421 residential sewage, urban runoff, animal feedlot operations, and fertilizer applications  
422 contributed 35%, 36%, 18%, and 5% of the non-point source TN loads and 76%, 10%,  
423 11%, and 1% of the NH<sub>4</sub>-N loads to the River Shaying of Central China. In spite of the  
424 differences in their natural and socioeconomic conditions, rural residential sewage was  
425 identified as the largest contributor of TN and NH<sub>4</sub>-N loads in all three basins, while  
426 animal feedlot operations and crop production activities were assessed to contribute  
427 moderately.

428 There have also been some studies that adopted an intermediate approach between  
429 the empirical coefficient methods and the process-based models to quantify N load  
430 contributions, For example, Wang *et al.* (2011) developed an ENPS\_LSB (estimate  
431 non-point source pollutant loads in a large-scale basin) model to take into account the  
432 complex non-point pollution sources (agricultural fields, urban, rural residential, and

433 livestock) in China. In this model, a number of factors such as transfer coefficient,  
434 natural correction factor, and social correction factor were introduced to correct the  
435 empirical export coefficients. Much different from the results of the aforementioned  
436 export coefficient studies, the application of the ENPS\_LSB model in the Yangtze River  
437 Basin estimated that 76.8% of non-point source dissolved TN loads were from  
438 agricultural fields. Chen et al. (2013) coupled a land-use based export coefficient model,  
439 a stream nutrient transport equation, and the Bayesian statistics for stream N source  
440 apportionment in the River ChangLe watershed of Zhejiang Province. They estimated  
441 that paddy fields, dry farming land, residential lands, and forest land contributed  
442 approximately 22%, 49%, 11%, and 18% of TN load for the entire watershed,  
443 respectively.

444 In this study, we identified crop production as the largest source of the TN load in  
445 the study region followed by septic tanks. TN loads from CAFOs and municipal sewage  
446 treatment plants varied between the third and fourth place seasonally. As for the  $\text{NH}_4\text{-N}$   
447 load, CAFOs, municipal sewage treatment plants, and industries were identified as the  
448 top three sources in the study region. Overall, our N load source attribution results are  
449 relatively consistent with previous studies that have incorporated nutrient transport in  
450 various ways, while much different from those studies purely based on export  
451 coefficients. One possible reason for the distinct difference between our study and those  
452 purely based on export coefficients is the incorporation of the N migration and  
453 transformation processes in the SWAT model. For example, although rural residential  
454 sewage may produce a large amount of TN and  $\text{NH}_4\text{-N}$  loads in the septic tanks due to  
455 the large rural population, they mostly migrated to the receiving water bodies through  
456 the long and slow process of groundwater movement, where many of which were  
457 reduced through physical, chemical, and biological processes. Failing to account for

458 these N transport and transformation processes could easily make the export coefficient  
459 method over-estimate both the TN and  $\text{NH}_4\text{-N}$  loads from rural residential sewage.

460 In addition, stable nitrogen ( $\delta^{15}\text{N}$ ) and oxygen ( $\delta^{18}\text{O}$ ) isotope data have been used  
461 to identify N sources in surface and groundwater based on different sources' distinct  
462 isotopic characteristics worldwide (Xue et al. 2009). In China, based on their monitored  
463  $^{15}\text{N}$  and  $\delta^{18}\text{O}$  values, Jin et al. (2015) concluded that the dominant sources of nitrate in  
464 surface water were soil nitrogen and chemical fertilizers in the West Lake watershed of  
465 eastern China. Ding et al. (2014) combined the dual isotope approach with a Bayesian  
466 model to identify diffusive nitrate sources in the Lake Taihu Basin of eastern China.  
467 They found that soil nitrogen and chemical fertilizers were the main source of nitrate  
468 throughout the year. Meanwhile, manure and sewage contributed 22.4% of nitrate  
469 during the dry season from October to April, compared to 17.8% in the rainy season  
470 from May to September. Using a similar approach in the ChangXing County of  
471 Zhejiang province, Yang et al. (2013) estimated that soil nitrogen and chemical  
472 fertilizers contributed approximately 71% of nitrate in surface water in May (wet season)  
473 compared to 24% by manure and sewage. Nevertheless, in December (dry season), they  
474 estimated that soil nitrogen and chemical fertilizers contributed around 38% compared  
475 to 54% by manure and sewage. This phenomenon of dominant contributions from soil  
476 nitrogen and chemical fertilizers in the wet season and increasing contribution  
477 proportions from manure and sewage in the dry season have also been reported in other  
478 regions of China, such as the Sanjiang Plain of northeastern China (Lu et al. 2015), the  
479 upper streams of Miyun Reservoir of northern China (Li et al. 2014), and the upper  
480 Yangtze River of southwestern China (Li et al. 2014), and they were consistent with our  
481 N load source attribution results in Fig. 4.

### 482 **3.5 Implications to N pollution control**

483 Five categories of water bodies have been specified in the Chinese Surface Water  
484 Quality Standard (GB3838-2002). Among them, category III water could be used for  
485 drinking, fishery, and swimming, while category V only for agriculture and scenery. Fig.  
486 6 compared the observed monthly TN and NH<sub>4</sub>-N concentrations at the Shakou Station  
487 between 2006 and 2011 with the Category III and V standards. Monthly NH<sub>4</sub>-N  
488 concentrations could meet the Category III standard except during two months in the  
489 first half of 2006. Monthly TN concentrations, however, were unable to meet the  
490 Category III standard throughout the period. In fact, less than 30% of the TN  
491 observations were able to meet the Category V standard. This suggests that the  
492 imminent focus of N pollution control in the region should lie in the reduction of TN  
493 load.

494 Our N source attribution results have suggested the need of a significant shift in the  
495 focus of N load reduction from the reliance of “end-of-pipe” sewage treatment facilities  
496 to an integrated watershed approach emphasizing stakeholder involvement and source  
497 prevention in the study region. Large but scattered settlements in many rural areas of  
498 China require a significant amount of investment in rural sewage treatment. Despite the  
499 recent developments in onsite wastewater treatment technologies, there remain  
500 considerable challenges in establishing an efficient system for rural sewage collection as  
501 well as treatment facility maintenance in China. It is therefore very hard to achieve large  
502 amount of N load reductions from rural households in the near future. Meanwhile, there  
503 have been many reports of excessive fertilizer application in different parts of China  
504 (Peng *et al.*, 2009; Zhang *et al.*, 2011; Yang *et al.*, 2012; Yan *et al.*, 2013). Previous  
505 surveys of the farmers in vicinity have revealed a prevalent lack of training in fertilizer  
506 applications and implementation of better fertilization practices such as soil testing and  
507 using controlled release fertilizers, as well as a sharp decline in applying organic

508 fertilizers (Yang and Fang, 2015). Considering its role as the largest TN load contributor  
509 and the prevalently inadequate fertilization practices, development of agricultural  
510 extension programs for encouraging better fertilization practices should be put in the top  
511 priority for reducing TN load in the region and possibly many other regions worldwide.

512 In addition, fixed locations and large operation scale made CAFOs another  
513 potential source for TN load reduction. The technologies of converting animal manure  
514 to biogas and organic fertilizers have been fairly mature (Nasir *et al.*, 2012). If designed  
515 and managed properly, the programs for reducing loads from CAFOs could not only  
516 reduce their TN load, but also mitigate the issue of lacking organic fertilizer  
517 applications in crop production. Therefore, developing sustainable agriculture programs  
518 and closing the nutrient loop in rural areas is the key to reducing TN load and improving  
519 water quality.

#### 520 **4. Conclusion**

521 The presence of multiple point and non-point pollution sources in a river basin is  
522 prevalent worldwide. Knowledge of their individual pollution load contributions and  
523 spatial-temporal patterns is essential to the development of sound river basin water  
524 pollution control strategies and programs. This study used the process-based SWAT  
525 model to analyze the N load source attributions as well as their spatiotemporal patterns  
526 for all known anthropogenic pollution sources in the Upper Huai River Basin of China.  
527 Key findings of the work are as follows:

528 - The process-based modeling approach can give more reliable pollutant load  
529 estimates and source attributions than the conventional approach based on empirical  
530 coefficients because the latter cannot account for the migration and transformation  
531 of the pollutants from the points of discharge to the final receiving water bodies.

532 Process-based models, therefore, should be used to simulate N loads from various



533 sources whenever the required data is available.

534 -The SWAT model driven by hourly rainfall inputs can enhance the representation of  
535 the hydrological processes of the study region, especially the sub-surface processes  
536 where nitrogen removal processes mostly take place. It outperformed the one driven  
537 by daily rainfall inputs for simulating both TN and  $\text{NH}_4\text{-N}$  loads.

538 - TN loads exhibited distinctive seasonal patterns. In general, TN loads from crop  
539 production were the largest, followed by septic tanks, municipal sewage treatment  
540 plants, and CAFOs. There was less seasonal variation in  $\text{NH}_4\text{-N}$  loads. In general,  
541  $\text{NH}_4\text{-N}$  loads from CAFOs were the largest, followed by industry, and municipal  
542 sewage treatment plants. Implementing sustainable agriculture programs for  
543 reducing loads from crop production and CAFOs and closing the nutrient loop in  
544 rural areas is the key to reducing TN load and improving water quality.

545 Eutrophication and other water problems caused by excessive nutrient discharge are  
546 issues of concern worldwide. Similar studies are very important to be undertaken for  
547 river basins in different parts of the world to help to estimate and prioritize the N loads  
548 from all anthropogenic pollution sources, and formulate the most appropriate strategies  
549 and programs for N pollution control. The model set up in this study can also be used to  
550 assess the impacts of land use and climate change on N loads and their uncertainties,  
551 and provide decision-support for the development of mitigation programs. In addition,  
552 due to limited water quality observations, we calibrated the SWAT models based on  
553 monthly TN and  $\text{NH}_4\text{-N}$  loads. In the future, water quality observations of higher  
554 temporal resolution (such as daily) could be used to derive more accurate contaminant  
555 load estimates for model calibration, better understand the temporal variability of  
556 contaminant loads from different pollution sources, and evaluate the impacts of climate  
557 change, especially extreme events, on contaminant loads and the associated

558 uncertainties.

### 559 **Acknowledgements**

560 The authors gratefully acknowledge the financial support provided by Chinese Natural  
561 Science Foundation (41201191), Chinese Ministry of Education New Faculty Fund  
562 (20120071120034), United Kingdom Royal Society – Chinese  
563 Natural Science Foundation Exchange Project (11311130117), and Fudan University  
564 Tyndall Center Project (FTC98503B04).

### 565 **References**

- 566 Abbaspour, K., 2011. SWAT-CUP4: SWAT calibration and uncertainty programs—a  
567 user manual. Swiss Federal Institute of Aquatic Science and Technology, Eawag.
- 568 Andersson, L., Rosberg, J., Pers, B.C., Olsson, J., Arheimer, B., 2005. Estimating  
569 catchment nutrient flow with the HBV-NP model: Sensitivity to input data. *AMBIO*.  
570 34 (7), 521-532.
- 571 Arnold, J.G., Allen, P.M. 1999. Automated methods for estimating baseflow and ground  
572 water recharge from streamflow records. *J Am Water Resour Assoc.* 35(2), 411-424.
- 573 Arnold, J.G., Moriasi, D.N., Gassman, P.W., Abbaspour, K.C., White, M.J., Srinivasan,  
574 R., Santhi, C., Harmel, R.D., Griensven, A.v., Liew, M.W.V., Kannan, N., Jha, M.K.,  
575 2014. SWAT: Model use, calibration, and validation. *Trans. ASABE.* 55 (4),  
576 1491-1508.
- 577 Carpenter, S., 2008. Phosphorus control is critical to mitigating eutrophication. *Proc.*  
578 *Natl. Acad. Sci. USA.* 105 (32), 11039–11040.
- 579 Cerro, I., Antiguada, I., Srinivasan, R., Sauvage, S., Volk, M., Sanchez-Perez, J.M.,  
580 2014. Simulating land management options to reduce nitrate pollution in an  
581 agricultural watershed dominated by an alluvial aquifer. *J. Environ. Qual.* 43 (1),  
582 67-74.

- 583 Chen, D.J., Lu, J., Huang, H., Liu, M., Gong, D.Q., Chen, J.B., 2013. Stream nitrogen  
584 sources apportionment and pollution control scheme development in an agricultural  
585 watershed in Eastern China. *Environ. Manage.* 52 (2), 450-466.
- 586 Delkash, M., Al-Faraj, F.A.M., Scholz, M., 2014. Comparing the export coefficient  
587 approach with the soil and water assessment tool to predict phosphorous pollution:  
588 The Kan Watershed case study. *Water Air Soil Pollut.* 225 (10), 60-69.
- 589 Ding, J.T., Xi, B.D., Gao, R.T., He, L.S., Liu, H.L., Dai, X.L., Yu, Y.J., 2014.  
590 Identifying diffused nitrate sources in a stream in an agricultural field using a dual  
591 isotopic approach. *Sci. Total Environ.* 484, 10-18.
- 592 Duncan, R., 2014. Regulating agricultural land use to manage water quality: The  
593 challenges for science and policy in enforcing limits on non-point source pollution in  
594 New Zealand. *Land Use Pol.* 41(4), 378-387.
- 595 Gallo, E.L., Meixner, T., Aoubid, H., Lohse, K.A., Brooks, P.D., 2015. Combined  
596 impact of catchment size, land cover, and precipitation on streamflow and total  
597 dissolved nitrogen: A global comparative analysis. *Glob. Biogeochem. Cycle.* 29 (7),  
598 1109-1121.
- 599 Galloway, J.N., Dentener, F.J., Capone, D.G., Boyer, E.W., Howarth, R.W., Seitzinger,  
600 S.P., Asner, G.P., Cleveland, C.C., Green, P.A., Holland, E.A., Karl, D.M., Michaels,  
601 A.F., Porter, J.H., Townsend, A.R., Vorosmarty, C.J., 2004. Nitrogen cycles: Past,  
602 present, and future. *Biogeochem.* 70 (2), 153-226.
- 603 Gassman, P.W., Sadeghi, A.M., Srinivasan, R., 2014. Applications of the SWAT model  
604 special section: Overview and insights. *J. Environ. Qual.* 43 (1), 1-8.
- 605 Guo, W.X., Fu, Y.C., Ruan, B.Q., Ge, H.F., Zhao, N.N., 2014. Agricultural non-point  
606 source pollution in the Yongding River Basin. *Ecolo. Indic.* 36 (1), 254-261.
- 607 Hao, S., Peng, W., Wu, W., Xu, J., 2014. Study on the spatial distribution of non-point

- 608 source pollution load in the Shaying River Basin (Chinese). *Yangtze River*. 45,  
609 6-9,13.
- 610 Henriksen, A., Hessen, D.O., Kessler, E., 1997. Nitrogen: A present and a future threat  
611 to the environment. *AMBIO*. 26 (5), 253-253.
- 612 Hou, J., Fan, B., Qu, B., Cai, L., Zhu, S., 2012. Reviews of the studies of the  
613 characteristics of rural domestic sewage discharge (Chinese). *J. Anhui Agri. Sci.* 40,  
614 964-967.
- 615 Howarth, R.W., 2008. Coastal nitrogen pollution: A review of sources and trends  
616 globally and regionally. *Harmful Algae*. 8 (1), 14-20.
- 617 Jiang, J.Y., Li, S.Y., Hu, J.T., Huang, J., 2014. A modeling approach to evaluating the  
618 impacts of policy-induced land management practices on non-point source pollution:  
619 A case study of the Liuxi River watershed, China. *Agric. Water Manage.* 131 (1),  
620 1-16.
- 621 Jin, Z.F., Qin, X., Chen, L.X., Jin, M.T., Li, F.L., 2015. Using dual isotopes to evaluate  
622 sources and transformations of nitrate in the West Lake watershed, Eastern China. *J.*  
623 *Contam. Hydrol.* 177, 64-75.
- 624 Lepisto, A., Granlund, K., Kortelainen, P., Raike, A., 2006. Nitrogen in river basins:  
625 Sources, retention in the surface waters and peatlands, and fluxes to estuaries in  
626 Finland. *Sci. Total Environ.* 365 (1-3), 238-259.
- 627 Li, C., Jiang, Y.B., Guo, X.Y., Cao, Y., Ji, H.B., 2014. Multi-isotope (N-15, O-18 and  
628 C-13) indicators of sources and fate of nitrate in the upper stream of Chaobai River,  
629 Beijing, China. *Environ. Sci.-Process Impacts*. 16 (11), 2644-2655.
- 630 Li, W.Z., Li, X.Y., Du, X.Z., Wang, X.X., 2014. Estimation of the nonpoint source  
631 nitrogen load in a strongly disturbed watershed of the North China Plain. *Water Sci.*  
632 *Technol.* 69 (6), 1304-1311.

- 633 Li, X.D., Liu, C.Q., Liu, X.L., Yu, J., Liu, X.Y., 2014. Sources and Processes Affecting  
634 Nitrate in a Dam-Controlled Subtropical River, Southwest China. *Aquat. Geochem.*  
635 20 (5), 483-500.
- 636 Lindgren, G., Wrede, S., Seibert, J., Wallin, M., 2007. Nitrogen source apportionment  
637 modeling and the effect of land-use class related runoff contributions. *Nord Hydrol.*  
638 38 (4-5), 317–331.
- 639 Lindstrom, G., Rosberg, J., Arheimer, B., 2005. Parameter precision in the HBV-NP  
640 model and impacts on nitrogen scenario simulations in the Ronnea River, Southern  
641 Sweden. *AMBIO* 34 (7), 533-537.
- 642 Liu, B., Liu, H., Zhang, B., Bi, J., 2013. Modeling nutrient release in the Tai Lake Basin  
643 of China: Source identification and policy implications. *Environ Manage.* 51 (3),  
644 724–737.
- 645 Lu, L., Cheng, H.G., Pu, X., Liu, X.L., Cheng, Q.D., 2015. Nitrate behaviors and source  
646 apportionment in an aquatic system from a watershed with intensive agricultural  
647 activities. *Environ. Sci.-Process Impacts.* 17 (1), 131-144.
- 648 Moriasi, D.N., Arnold, J.G., Van Liew, M.W., Bingner, R.L., Harmel, R.D., Veith, T.L.,  
649 2007. Model evaluation guidelines for systematic quantification of accuracy in  
650 watershed simulations. *Trans. ASABE* . 50 (3), 885-900.
- 651 Nash, J.E., Sutcliffe, J.V., 1970. River flow forecasting through conceptual models part I  
652 - A discussion of principles. *J. Hydrol.* 10, 282-290.
- 653 Nasir, I.M., Ghazi, T.I.M., Omar, R., 2012. Anaerobic digestion technology in livestock  
654 manure treatment for biogas production: A review. *Eng. Life Sci.* 12 (3), 258–269.
- 655 Nasr, A., Bruen, M., Jordan, P., Moles, R., Kiely, G., Byrne, P., 2007. A comparison of  
656 SWAT, HSPF and SHETRAN/GOPC for modelling phosphorus export from three  
657 catchments in Ireland. *Water Res.* 41 (5), 1065-1073.

- 658 Oliver, C.W., Radcliffe, D.E., Risse, L.M., Habteselassie, M., Mukundan, R., Jeong, J.,  
659 Hoghooghi, N., 2014. Quantifying the contribution of on-site wastewater treatment  
660 systems to stream discharge using the SWAT model. *J. Environ. Qual.* 43 (2),  
661 539-548.
- 662 Ouyang, W., Song, K.Y., Wang, X.L., Hao, F.H., 2014. Non-point source pollution  
663 dynamics under long-term agricultural development and relationship with landscape  
664 dynamics. *Ecol. Indic.* 45(5), 579-589.
- 665 Panagopoulos, Y., Gassman, P.W., Arritt, R.W., Herzmann, D.E., Campbell, T.D., Jha,  
666 M.K., Kling, C.L., Srinivasan, R., White, M., Arnold, J.G., 2014. Surface water  
667 quality and cropping systems sustainability under a changing climate in the Upper  
668 Mississippi River Basin. *J. Soil Water Conserv.* 69 (6), 483-494.
- 669 Pastuszak, M., Kowalkowski, T., Kopinski, J., Stalenga, J., Panasiuk, D., 2014. Impact  
670 of forecasted changes in Polish economy (2015 and 2020) on nutrient emission into  
671 the river basins. *Sci. Total Environ.* 493, 32-43.
- 672 Pease, L.M., Oduor, P., Padmanabhan, G., 2010. Estimating sediment, nitrogen, and  
673 phosphorous loads from the Pipestem Creek watershed, North Dakota, using  
674 AnnAGNPS. *Comput. Geosci.* 36, 282-291.
- 675 Peng, S.B., Tang, Q.Y., Zou, Y.B., 2009. Current status and challenges of rice  
676 production in China. *Plant Prod. Sci.* 12 (1), 3-8.
- 677 Prescott, J.A., 1940. Evaporation from water surface in relation to solar radiation. *Trans.*  
678 *R. Soc. S. Aust.* 40, 114-118.
- 679 Que, Z., Seidou, O., Droste, R.L., Wilkes, G., Sunohara, M., Topp, E., Lapen, D.R.,  
680 2015. Using AnnAGNPS to predict the effects of tile drainage control on nutrient and  
681 sediment loads for a river basin. *J. Environ. Qual.* 44, 629-641.
- 682 Rankinen, K., Karvonen, T., Butterfield, D., 2006. An application of the GLUE

- 683 methodology for estimating the parameters of the INCA-N model. *Sci. Total Environ.*  
684 365, 123-139.
- 685 Saxton, K.E., Willey, P.H. (Eds.), 2005. *The SPAW model for agricultural field and*  
686 *pond hydrologic simulation.* CRC Press LLC.
- 687 Shen, Z.Y., Chen, L., Ding, X.W., Hong, Q., Liu, R.M., 2013. Long-term variation  
688 (1960-2003) and causal factors of non-point-source nitrogen and phosphorus in the  
689 upper reach of the Yangtze River. *J. Hazard Mater.* 252-253 (10), 45-56.
- 690 Shi, X.Z., Yu, D.S., Xu, S.X., Warner, E.D., Wang, H.J., Sun, W.X., Zhao, Y.C., Gong,  
691 Z.T., 2010. Cross-reference for relating genetic soil classification of China with  
692 WRB at different scales. *Geoderma.* 155, 344-350.
- 693 Vitousek, P.M., Cassman, K., Cleveland, C., Crews, T., Field, C.B., Grimm, N.B.,  
694 Howarth, R.W., Marino, R., Martinelli, L., Rastetter, E.B., Sprent, J.I., 2002.  
695 Towards an ecological understanding of biological nitrogen fixation. *Biogeochem.* 57  
696 (1), 1-45.
- 697 Wade, A.J., Butterfield, D., Whitehead, P.G., 2006. Towards an improved understanding  
698 of the nitrate dynamics in lowland, permeable river-systems: Applications of  
699 INCA-N. *J. Hydrol.* 330 (1-2), 185-203.
- 700 Wang, J., Chen, J., Fu, Y., Yang, T., 2010. Survey of the rural sewage discharge in the  
701 key watersheds of Sichuan Province (Chinese). *Guangdong Agri. Sci.* 37, 150-152.
- 702 Wang, S., Qian, X., Zhao, G., Zhang, W., Zhao, Y., Fan, Z., 2013. Contribution analysis  
703 of pollution sources around the Dianshan Lake (Chinese). *Resour. Environ. Yangtze*  
704 *Basin.* 22, 331-336.
- 705 Wang, X., Hao, F.H., Cheng, H.G., Yang, S.T., Zhang, X., Bu, Q.S., 2011. Estimating  
706 non-point source pollutant loads for the large-scale basin of the Yangtze River in  
707 China. *Environ. Earth Sci.* 63 (5), 1079-1092.

- 708 Wang, Y., Fang, Y., Jiao, J., 2008. Evaluation of the sewage treatment performance of  
709 the septic tanks in the rural areas of Jiangsu Province (Chinese). *J. Ecol. Rural*  
710 *Environ.* 24, 80-83.
- 711 Withers, P.J.A., May, L., Jarvie, H.P., Jordan, P., Doody, D., Foy, R.H., Bechmann, M.,  
712 Cooksley, S., Dils, R., Deal, N., 2012. Nutrient emissions to water from septic tank  
713 systems in rural catchments: Uncertainties and implications for policy. *Environ. Sci.*  
714 *Policy.* 24, 71-82.
- 715 Wu, Y.P., Chen, J., 2013. Investigating the effects of point source and nonpoint source  
716 pollution on the water quality of the East River (Dongjiang) in South China. *Ecol.*  
717 *Indic.* 32, 294-304.
- 718 Xie, H., Lian, Y.Q., 2013. Uncertainty-based evaluation and comparison of SWAT and  
719 HSPF applications to the Illinois River Basin. *J. Hydrol.* 481, 119-131.
- 720 Xu, H., Lu, X., Li, X., Jin, Z., 2008. Investigation of the quantity and quality of rural  
721 sewage discharge in the Lake Tai Basin (Chinese). *Henan Sci.* 26, 854-857.
- 722 Xu, H., Yang, L.Z., Zhao, G.M., Jiao, J.G., Yin, S.X., Liu, Z.P., 2009. Anthropogenic  
723 impact on surface water quality in Taihu Lake region, China. *Pedosphere.* 19,  
724 765-778.
- 725 Xue, D.M., Botte, J., De Baets, B., Accoe, F., Nestler, A., Taylor, P., Van Cleemput, O.,  
726 Berglund, M., Boeckx, P., 2009. Present limitations and future prospects of stable  
727 isotope methods for nitrate source identification in surface- and groundwater. *Water*  
728 *Res.* 43 (5), 1159-1170.
- 729 Yan, Z., Liu, P., Li, Y., Ma, L., Alva, A., Dou, Z., Chen, Q., Zhang, F., 2013. Phosphorus  
730 in China's intensive vegetable production systems: Overfertilization, soil enrichment,  
731 and environmental implications. *J. Environ. Qual.* 42, 982-989.
- 732 Yang, L.P., Han, J.P., Xue, J.L., Zeng, L.Z., Shi, J.C., Wu, L.S., Jiang, Y.H., 2013.



- 733 Nitrate source apportionment in a subtropical watershed using Bayesian model. *Sci.*  
734 *Total Environ.* 463, 340-347.
- 735 Yang, X., Fang, S., 2015. Practices, perceptions, and implications of fertilizer use in  
736 East-Central China. *AMBIO*. DOI 10.1007/s13280-015-0639-7.
- 737 Yang, X., Fang, S., Lant, C.L., Luo, X., Zheng, Z., 2012. Overfertilization in the  
738 economically developed and ecologically critical Lake Tai Region, China. *Human*  
739 *Ecol.* 40 (6), 957-964.
- 740 Yang, X., Liu, Q., He, Y., Luo, X., Zhang, X., 2015. Comparison of daily and sub-daily  
741 SWAT models for daily streamflow simulation in the Upper Huai River Basin of  
742 China. *Stoch. Environ. Res. Risk. Assess.* DOI 10.1007/s00477-015-1099-0.
- 743 Yu, D.S., Shi, X.Z., Wang, H.J., Sun, W.X., Liu, Q.H., Zhao, Y.C., 2007a. Regional  
744 patterns of soil organic carbon storages in China. *J. Environ. Manage.* 85, 680-689.
- 745 Yu, D.S., Shi, X.Z., Wang, H.J., Sun, W.X., Warner, E.D., Liu, Q.H., 2007b. National  
746 scale analysis of soil organic carbon storage in China based on Chinese soil  
747 taxonomy. *Pedosphere* 17, 11-18.
- 748 Yun, S.L., Ahn, J.H., Min, K.S., Chu, K.H., Um, C.Y., Ko, K.B., 2015. Non-point  
749 sources of pollution from cultivated lands in river districts and their contribution to  
750 water bodies along the North Han River Basin in Korea. *Desalin. Water Treat.* 53,  
751 2301-2311.
- 752 Zhang, P., Liu, Y.H., Pan, Y., Yu, Z.R., 2013. Land use pattern optimization based on  
753 CLUE-S and SWAT models for agricultural non-point source pollution control. *Math.*  
754 *Comput. Model.* 58, 588-595.
- 755 Zhang, P.P., Liu, R.M., Bao, Y.M., Wang, J.W., Yu, W.W., Shen, Z.Y., 2014. Uncertainty  
756 of SWAT model at different DEM resolutions in a large mountainous watershed.  
757 *Water Res.* 53, 132-144.

- 758 Zhang, Y., Luan, S., Chen, L., Shao, M., 2011. Estimating the volatilization of ammonia  
759 from synthetic nitrogenous fertilizers used in China. *J. Environ. Manage.* 92,  
760 480–493.
- 761 Zuo, D., Wang, Y., Chen, J., 1963. Regional spatial patterns of solar radiation in China  
762 (Chinese). *ACTA Meterol. SINICA.* 33, 78-95.

ACCEPTED MANUSCRIPT

**Table 1.** Data inputs for the SWAT model

Category	Data	Scale/Extent	Data Sources
	DEM	1:50,000	Chinese National Geomatics Center
	Land Use/ Land Cover (2005)	1:100,000	Chinese Academy of Sciences
	Soil types and soil properties	1:1000,000	Nanjing Institute of Soil Science; Henan Province Soil Survey Office (1995); SPAW software
Water Quantity	River networks	1:250,000	Chinese Academy of Sciences
	Daily weather (1960-2011)	1 station	China Meteorological Administration
	Daily and hourly rainfall (2001-2011)	28 stations	Ministry of Water Resources of China
	Monthly streamflow (2005-2011)	3 stations	Ministry of Water Resources of China
	Daily reservoir outflow (2005-2011)	3 reservoirs	Ministry of Water Resources of China
	Water Quality	Annual N emissions from industries (2010)	74 river segments
Annual N emissions from CAFOs (2010)		74 river segments	2010 Census of Pollution Sources in the Zhumadian City
Annual N emissions from municipal sewage treatment plants (2010)		6 sewage treatment plants	Bureau of Environmental Protection of the Zhumadian City
Annual N emissions from SAFOs (2010)		9 counties and 1 district	Bureau of Animal Husbandry of the Zhumadian City
Total rural population (2010)		9 counties and 1 district	Statistical Yearbook of the Zhumadian City
Total crop planting areas (2010)		9 counties and 1 district	Statistical Yearbook of the Zhumadian City
Crop management practices		116 farmers	Field Survey

**Table 2.** Crop management operations during the wheat-corn rotation

Crop	Year	Month	Day	Operations
Corn	1	6	4	Start growth season
	1	6	4	Apply compound fertilizers (750 kg/ha)
	1	6	4	Apply urea (187.5 kg/ha)
	1	7	6	Apply urea (150 kg/ha)
	1	9	30	Harvest
Wheat	1	10	7	Start growth season
	1	10	7	Apply compound fertilizers (750 kg/ha)
	1	10	7	Apply urea (93.75 kg/ha)
	2	2	10	Apply urea (93.75 kg/ha)
	2	6	1	Harvest

**Table 3.** Comparison of parameter values between the daily and hourly SWAT models for discharge simulation

Parameter	Description	Range	Calibrated Values	
			Daily Model	Hourly Model
SURLAG	Surface runoff lag coefficient	1-10	7.8	8.7
ALPHA_BF	Baseflow alpha factor	0.03-0.1	0.06	0.06
GW_DELAY	Groundwater delay	10-300	13.8	265.1
GWQMN	Threshold depth of water in the shallow aquifer required for return flow to occur	10-150	26.7	72.8
REVAPMN	Threshold depth of water in the shallow aquifer for "revap" to occur	10-200	134.2	18.6
GW_REVAP	Groundwater "revap" coefficient	0.02-0.2	0.02	0.15
CANMX_AGR	Maximum canopy storage of agricultural land	1-10	1.4	1.3
CANMX_URML	Maximum canopy storage of medium/low density residential areas	1-10	0.3	2.4
EPCO	Plant uptake compensation factor	0.85-1	0.90	0.91
ESCO	Soil evaporation compensation factor	0.85-1	0.87	1.00
CN2_AGR	Moisture condition II curve number for agricultural land	67-99	69-91 <sup>a</sup>	76-98
CN2_URML	Moisture condition II curve number for medium/low density residential areas	62-92	60-75 <sup>a</sup>	75-90
CH_N2	Manning's "n" value for the main channel	0.035-0.049	0.045	0.042
CH_K2	Effective hydraulic conductivity in main channel alluvium	0-50	6.6	4.9
SOL_AWC	Available water capacity of the soil layer	0.12-0.36	0.15-0.35 <sup>b</sup>	0.15-0.35
SOL_K	Saturated hydraulic conductivity of the soil layer	1.6-901.3	1.9-862.8 <sup>b</sup>	1.9-864.0
CH_N1	Manning's "n" value for the tributary channels	0.19-0.32	0.27	0.24
CH_K1	Effective hydraulic conductivity in tributary channel alluvium	0-50	3.7	0.9

<sup>a</sup> Show the range of the calibrated values for different hydrological groups.

<sup>b</sup> Show the range of the calibrated values for different soil types and soil layers.

**Table 4.** Comparison of parameter values and sensitivities between the daily and sub-daily SWAT models

Parameter	Description	Range	Calibrated Values	
			Daily Model	Hourly Model
CDN	Denitrification exponential rate coefficient	0-3	2.38	2.22
CMN	Rate factor for humus mineralization of active organic nitrogen	0.001-0.003	0.0018	0.0013
NPERCO	Nitrogen percolation coefficient	0-1	0.1	0.1
RSDCO	Residue decomposition coefficient	0.02-0.1	0.08	0.06
ERORGN	Organic N enrichment ratio	0-5	0.28	0.69
COEFF_DENITR	Denitrification rate coefficient	0.1-50	14.2	37.9
COEFF_NITR	Nitrification rate coefficient	0.1-300	20.4	83.5
BC1	Rate constant for biological oxidation of NH <sub>4</sub> to NO <sub>2</sub> in the reach at 20°C	0.1-1	0.81	0.98
BC3	Rate constant for hydrolysis of organic N to NH <sub>4</sub> in the reach at 20°C	0.02-0.4	0.33	0.27
RS1	Local algal settling rate in the reach at 20°C	0.15-1.82	0.99	0.60
RS4	Rate coefficient for organic N settling in the reach at 20°C	0.001-0.1	0.08	0.07
AI0	Ratio of chlorophyll-a to algal biomass	10-100	52.66	55.40
K_N	Michaelis-Menton half-saturation constant for nitrogen	0.01-0.3	0.09	0.17
MUMAX	Maximum specific algal growth rate at 20°C	1-3	2.27	2.88
P_N	Algal preference factor for ammonia	0-1	0.88	0.59
RHOQ	Algal respiration rate at 20°C	0.05-0.5	0.10	0.37

**Table 5.** Comparison of model evaluation statistics between the daily and hourly SWAT models for discharge and N load simulations

Station	NSE				R <sup>2</sup>			
	Calibration		Validation		Calibration		Validation	
	Daily	Hourly	Daily	Hourly	Daily	Hourly	Daily	Hourly
Discharge								
Lixin	0.92	0.86	0.84	0.94	0.92	0.89	0.93	0.97
Luzhuang	0.85	0.82	0.84	0.83	0.89	0.94	0.87	0.87
Shakou	0.98	0.93	0.95	0.98	0.99	0.96	0.98	0.98
TN load								
Shakou	0.63	0.82	--	--	0.77	0.87	--	--
NH <sub>4</sub> -N load								
Shakou	0.58	0.82	--	--	0.80	0.84	--	--

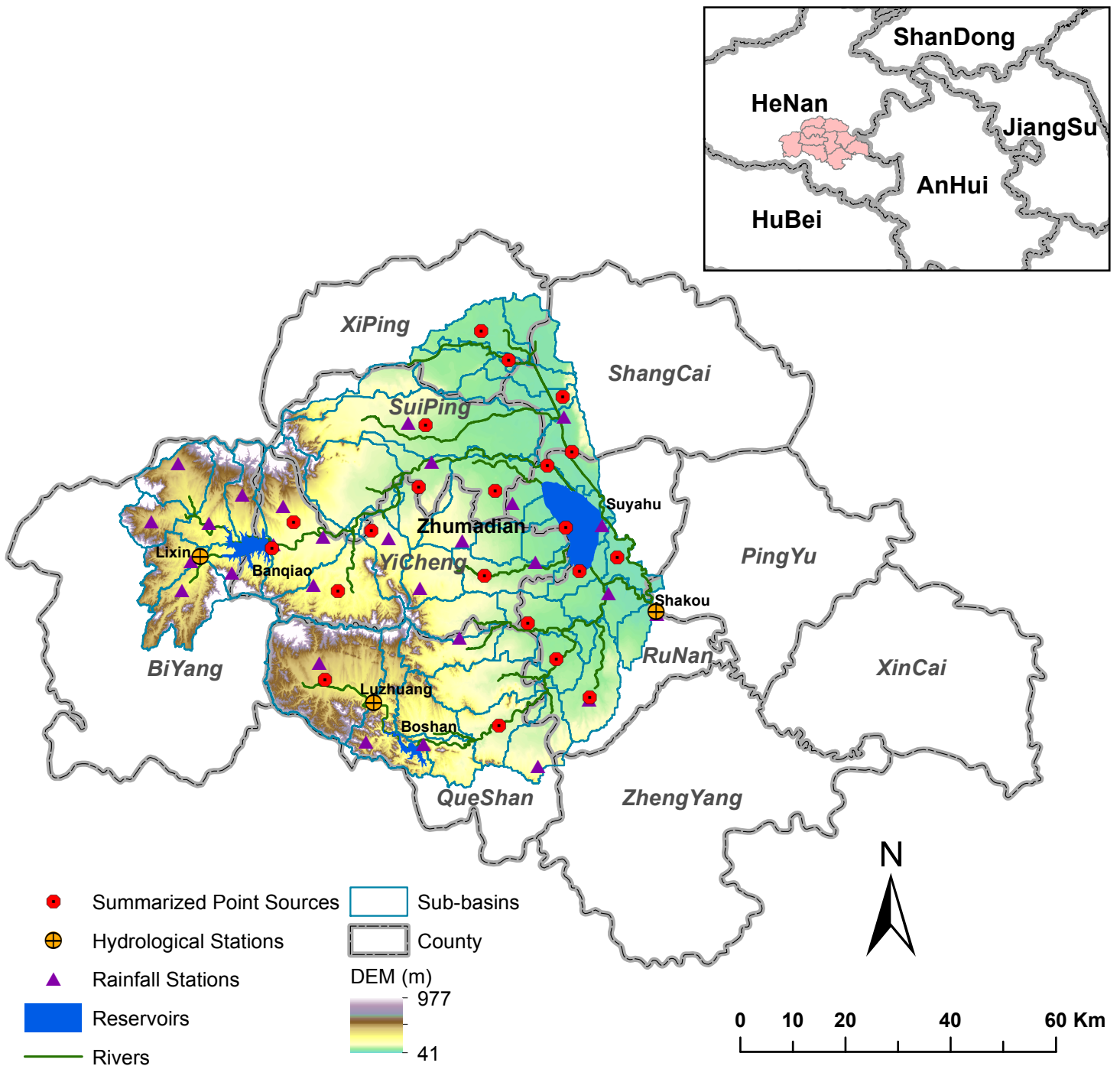


Fig. 1 - The map of the study region. Out of 55 sub-basins, 21 of them have point sources of N. The location of the administrative boundary of the Zhumadian City overlapped on the map of adjacent provinces is shown in the upper right panel.



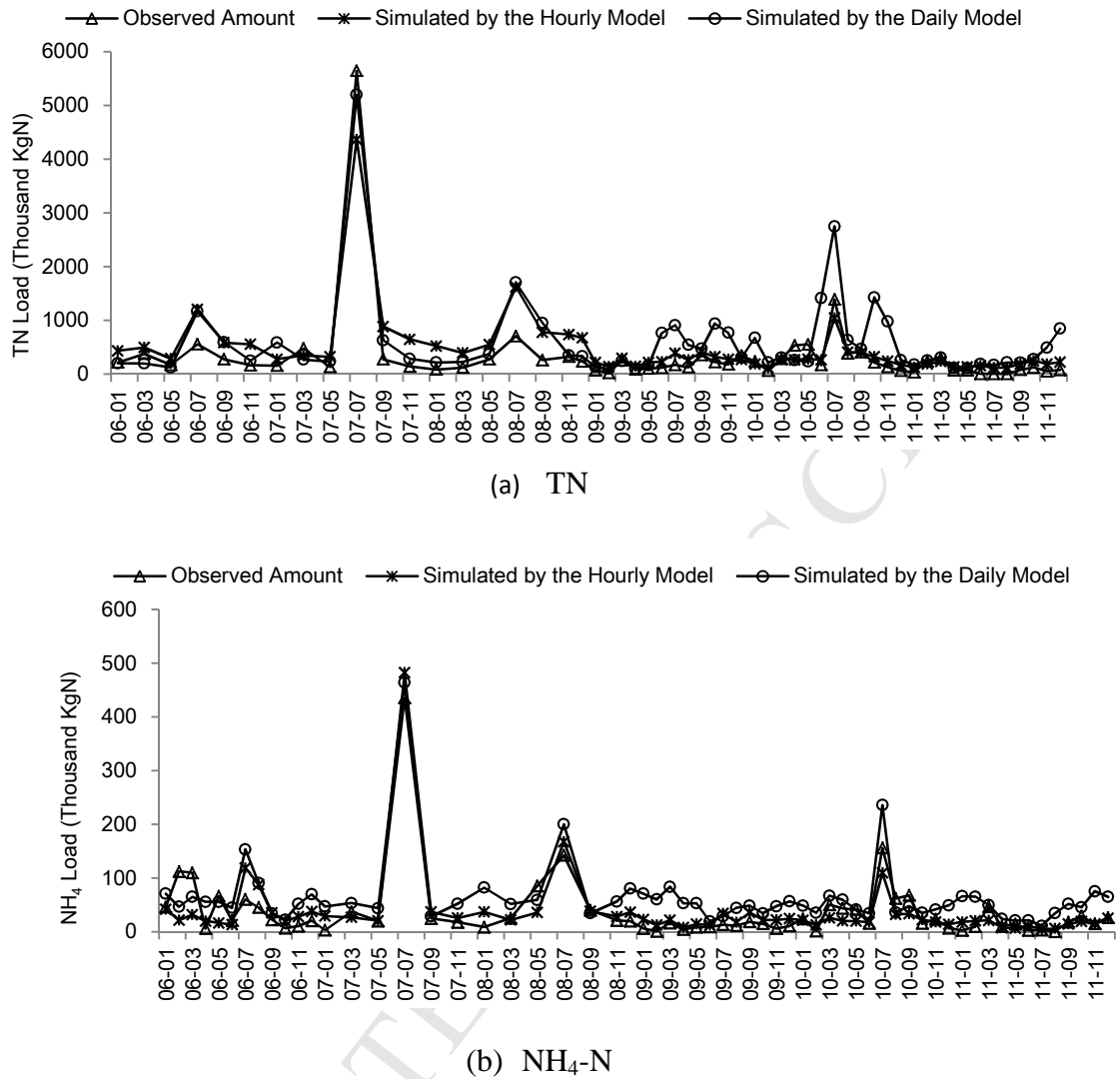


Fig. 2. The observed and simulated amount of monthly N loads by the daily and hourly SWAT models for the period 2006-2011 at the Shakou station: (a) TN; (b)

NH<sub>4</sub>-N

ID	Downstream Distance (km)	Contribution Area (km <sup>2</sup> )
1	20	333
2	43	1069
3	53	1323
4	64	1436
5	78	1806
6	109	1821
7	120	2330
8	130	4481
9	146	5803

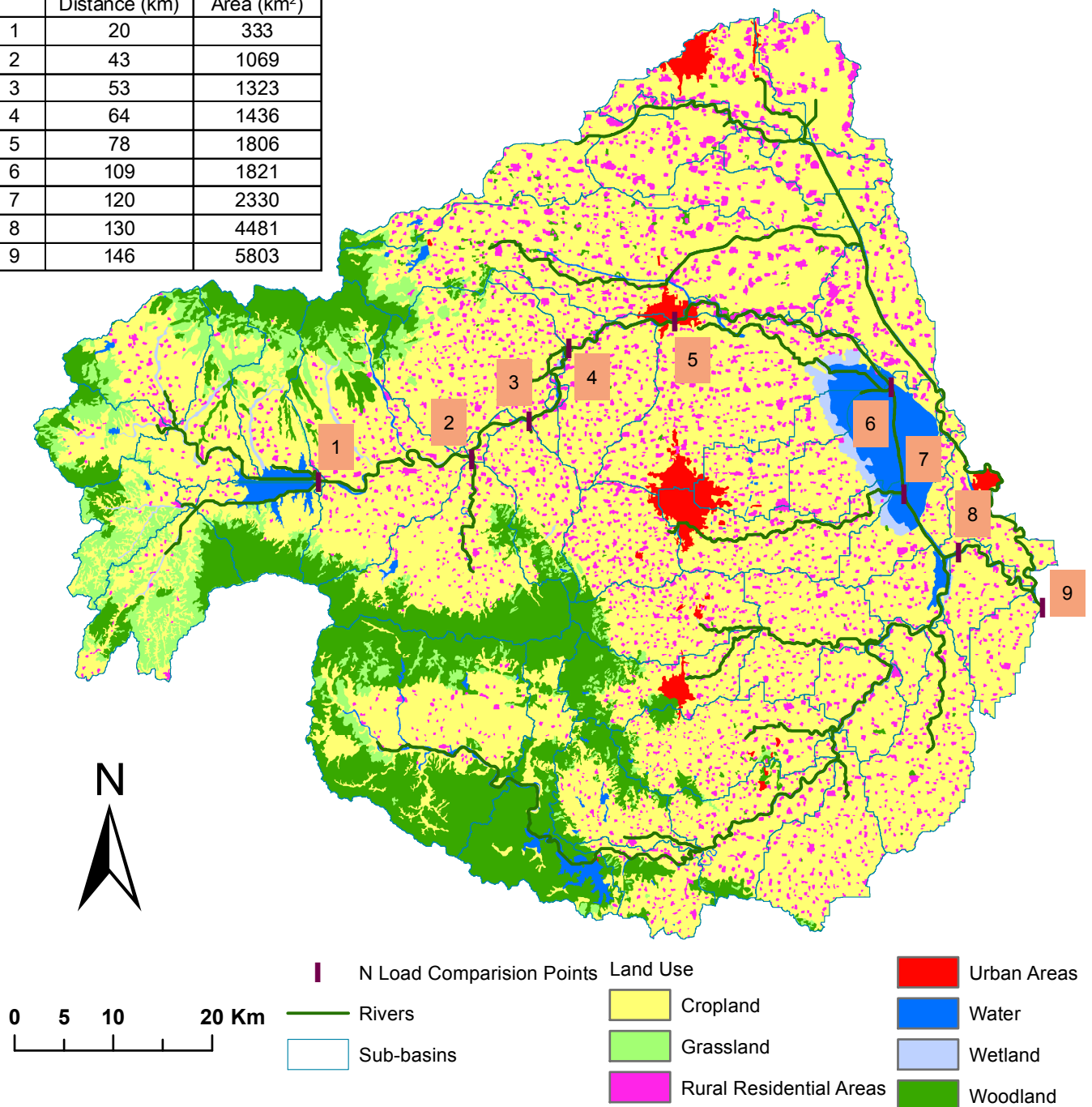


Fig. 3 - Locations of nine sub-basin outlets along the main reach of the Ru River for comparing TN and NH<sub>4</sub>-N loads

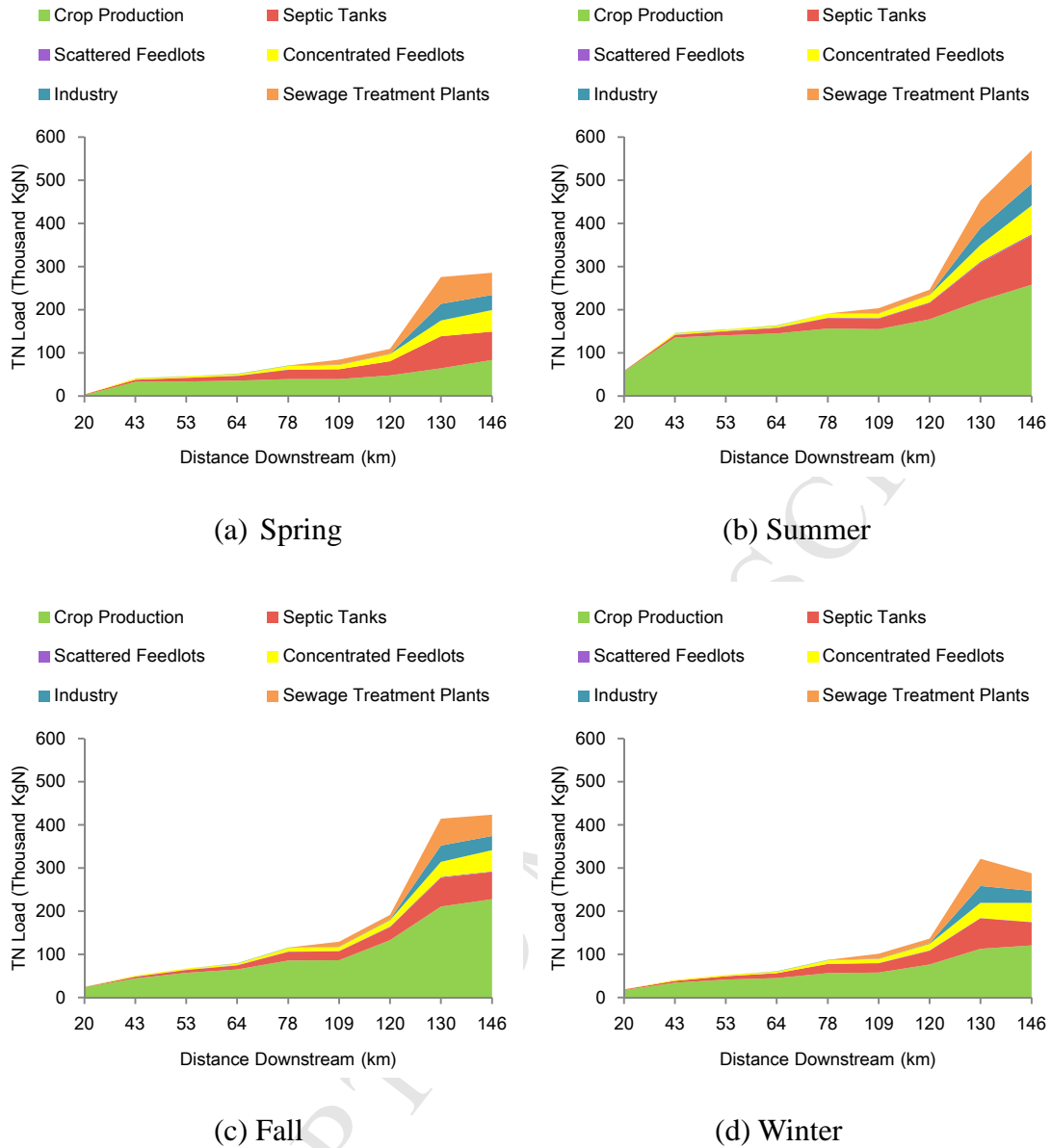


Fig. 4- Average monthly TN load from various pollution sources along the main reach of the Ru River in four seasons between 2006 and 2011: (a) Spring; (b) Summer; (c) Fall; and (d) Winter.

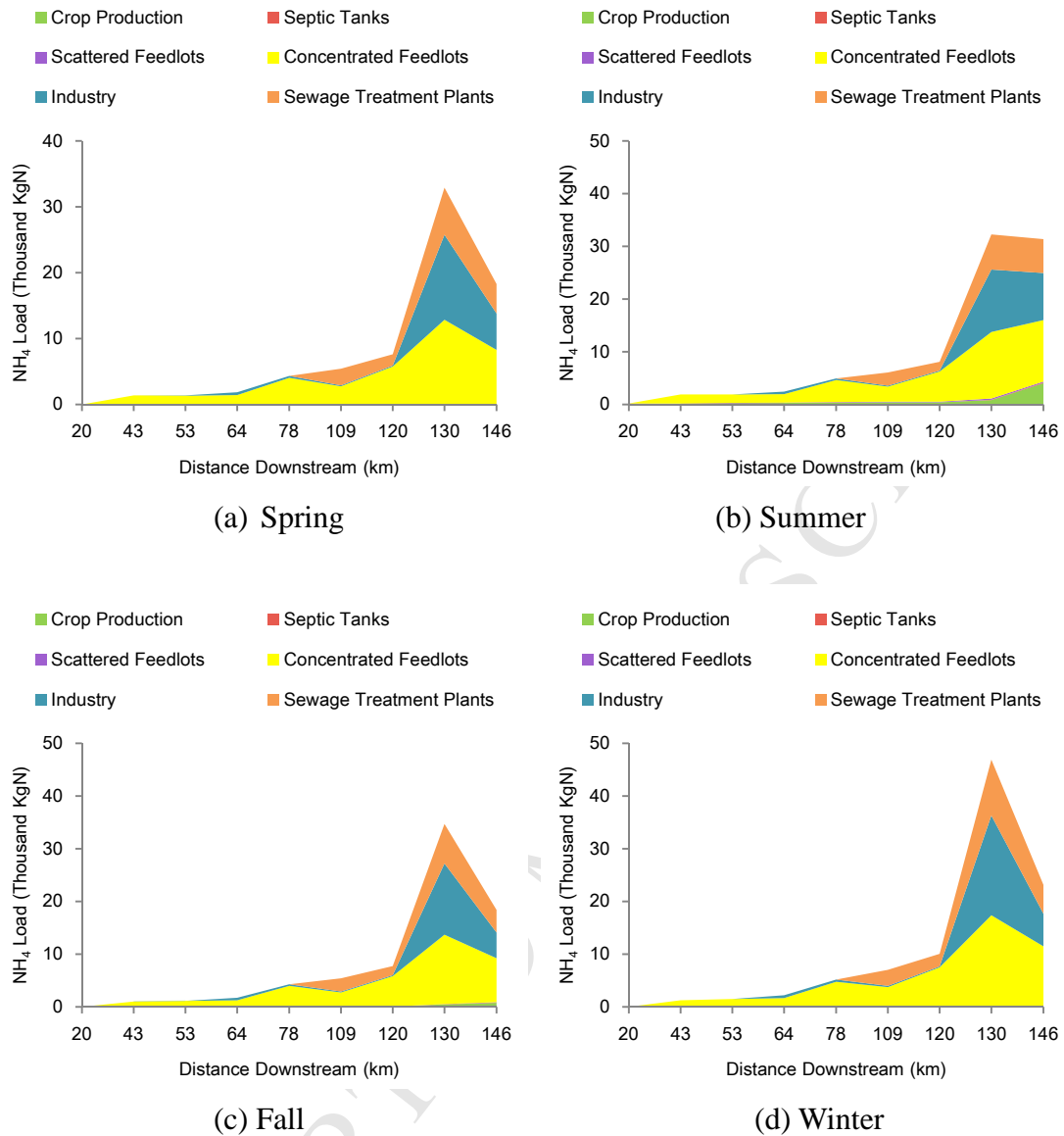
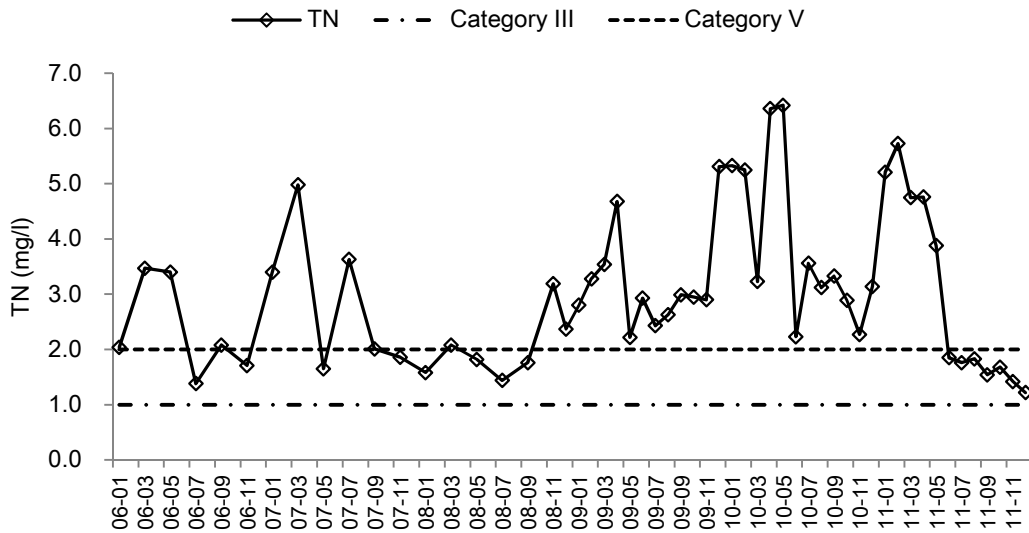
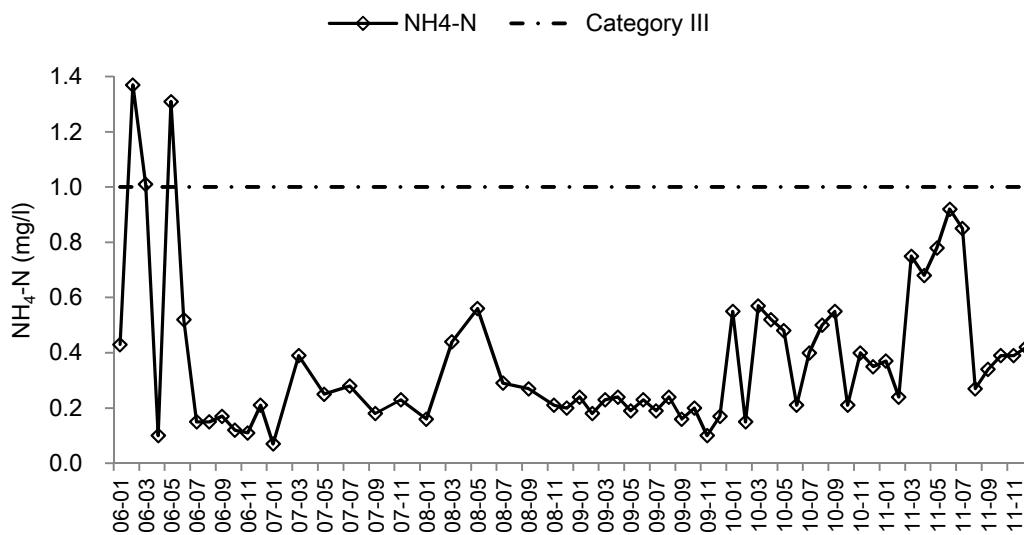


Fig. 5- Average monthly  $\text{NH}_4\text{-N}$  load from various pollution sources along the main reach of the Ru River in four seasons between 2006 and 2011: (a) Spring; (b) Summer; (c) Fall; and (d) Winter.



(a) TN

(b) NH<sub>4</sub>-NFig. 6- Monthly TN and NH<sub>4</sub>-N concentrations at the outlet of the Ru River Basin

**Highlights**

- 1) The SWAT models simulate N loads from all known anthropogenic pollution sources.
- 2) The SWAT models with daily and hourly rainfall are compared in N load simulation.
- 3) TN load from crop production is the largest followed by septic tanks in the basin.
- 4)  $\text{NH}_4\text{-N}$  load from concentrated feedlot operations is the largest in the basin.